



HAL
open science

The histone acetyltransferases CBP/p300 are degraded in NIH 3T3 cells by activation of Ras signalling pathway

Sara Sánchez-Molina, José L Oliva, Susana García-Vargas, Ester Valls, José M Rojas, Marian A Martínez-Balbás, Marian A Martínez-Balbás

► To cite this version:

Sara Sánchez-Molina, José L Oliva, Susana García-Vargas, Ester Valls, José M Rojas, et al.. The histone acetyltransferases CBP/p300 are degraded in NIH 3T3 cells by activation of Ras signalling pathway. *Biochemical Journal*, 2006, 398 (2), pp.215-224. 10.1042/BJ20060052 . hal-00478509

HAL Id: hal-00478509

<https://hal.science/hal-00478509>

Submitted on 30 Apr 2010

HAL is a multi-disciplinary open access archive for the deposit and dissemination of scientific research documents, whether they are published or not. The documents may come from teaching and research institutions in France or abroad, or from public or private research centers.

L'archive ouverte pluridisciplinaire **HAL**, est destinée au dépôt et à la diffusion de documents scientifiques de niveau recherche, publiés ou non, émanant des établissements d'enseignement et de recherche français ou étrangers, des laboratoires publics ou privés.

The histone acetyltransferases CBP/p300 are degraded in NIH3T3 cells by activation of Ras signaling pathway

Sara Sánchez-Molina*, José Luis Oliva†, Susana García-Vargas†, Ester Valls*, José M. Rojas† and Marian A. Martínez-Balbás*‡

*Instituto de Biología Molecular de Barcelona. CID. Consejo Superior de Investigaciones Científicas (CSIC). Parc Científic de Barcelona (PCB). Josep Samitier 1-5. 08028 Barcelona. Spain

†Unidad de Biología Celular. Centro Nacional de Microbiología. Instituto de Salud Carlos III. 28220 Majadahonda, Madrid, Spain.

Short Title: Activation of Ras pathway induces loss of CBP/p300

Key words: CBP/p300/ HAT activity/ acetylation/ NIH3T3 / Ras pathway/ Mdm2

‡Corresponding author

Marian A. Martínez-Balbás

Instituto de Biología Molecular de Barcelona. CID.

Consejo Superior de Investigaciones Científicas (CSIC).

Parc Científic de Barcelona (PCB).

Josep Samitier 1-5.

08028 Barcelona.

SPAIN

E-mail: mmbbmc@ibmb.csic.es

Tel.: 34-93-403-49-61

Fax: 34-93- 403-49-79

ABSTRACT

The CBP and p300 (CBP/p300) acetyltransferases function as transcriptional co-activators and play critical roles in cell differentiation and proliferation. Accumulating evidence shows that alterations of the p300 and CBP (CBP/p300) protein levels are linked to human tumors. In the present study, we show that the levels of the CBP and p300 co-activators decrease dramatically by continuous PDGF and Ras signaling pathway activation in NIH 3T3 fibroblasts. This effect occurs by reducing the expression levels of the CBP and p300 genes. In addition, CBP and p300 are degraded by the 26S proteasome pathway leading to an overall decrease in the levels of the CBP and p300 proteins. Furthermore, we provide evidence that Mdm2, in the presence of active H-Ras or N-Ras induces CBP/p300 degradation in NIH3T3 cells. These findings support a novel mechanism for modulating other signaling transduction pathways that require these common co-activators.

INTRODUCTION

For many years, acetylation of the histone N-terminal tails has been associated with transcriptional activation (1). Histone acetylation is performed by histone acetyltransferases (HATs), while the reversed deacetylation process is conducted by histone deacetylases (HDACs) (2). Different HAT families have been characterized among CBP and p300, the GNAT super family, the MYST family, nuclear receptor co-activators, TAF II 250 and the TFIIC family (2). The global co-activators CBP and p300 not only exhibit histone acetyltransferase activity (3, 4), but they also acetylate non-histone proteins, such as transcription factors (5-10), thereby highlighting the potential importance of HAT activity in CBP/p300 function. CBP/p300 also acts as a transcriptional co-activator (11, 12), by binding numerous transcription factors. Viral oncoproteins, such as SV40 T antigen or E1A also specifically target these proteins (13). As transcriptional co-activators, CBP/p300 are involved in multiple signal-dependent transcriptional events. Many signals from the environment are thought to induce gene transcription by activating intracellular biochemical pathways (Ras, BMP, TGF-B, etc), which control the ability of transcription factors to recruit CBP/p300 to specific promoters. CBP and p300 have been postulated to integrate the different signals of gene expression by serving as essential co-factors of STAT1, Smad, AP-1, and c-Myc transcription factors. In this way, they modulate gene-specific responses to simultaneous activation of two or more signaling transduction pathways, driven by competing transcription factors based on limiting amounts of CBP/p300 (14). Given that many transcriptional activators, which respond to different cellular pathways, can recruit CBP/p300 to a promoter, control of either CBP/p300 protein levels (by regulating CBP/p300 mRNA levels or protein degradation) and/or CBP/p300 activity may be of general importance for signal-regulated transcription

Ras proteins operate as molecular switches in signal transduction cascades controlling cell proliferation, differentiation, or apoptosis, and, like all G proteins, are controlled by a regulated GTP/GDP cycle (15). The mammalian genome contains three *ras* genes that encode highly related proteins of 21 kDa termed H-Ras, N-Ras and K-Ras with its two variants, K-Ras4A and K-Ras4B, generated from two alternative fourth exons. Each of the three human *ras* proto-oncogenes can give rise to a transforming

oncogene *via* single base mutations. Mutations at codons 12, 13 or 61 significantly downgrade the GTPase ability of the resulting mutant Ras proteins, which are thus rendered constitutively active and able to transform mammalian cells. Once activated, Ras proteins interact with effector proteins, mainly Raf, PI3K and Ral-GDS (16), resulting in the activation of downstream signaling pathways, such as the Raf/MEK/ERK, PI3K/AKT or the Ral-GDS/Ral A pathway (17, 18) ultimately leading to the transcriptional activation of genes (15). The high degree of sequence homology, coupled with the essentially identical capability of mutated forms of H-Ras, the two K-Ras isoforms (4A and 4B) and N-Ras to cause transformation of NIH3T3 fibroblasts and other cell types, supports the idea that all Ras proteins have the same role *in vivo*. However, growing evidence suggests the possibility of non-redundant roles for the three Ras homologues (15, 18-20). The embryonic lethality seen in the *Kras*, but not *Hras* or *Nras*, knockout mice also lends credence to this idea (21).

Furthermore, CBP/p300 genes are altered in various human tumors (22, 23), which is consistent with studies on CBP +/- mice suggesting that CBP works as a tumor suppressor in the hematopoietic system (24). Moreover, human patients with Rubinstein-Taybi syndrome (RTS), which results from CBP heterozygosity, also experience an increased incidence of malignancy (25, 26). The profound effects of CBP/p300 suppression, both in cell culture and in intact animals (24) allow us to predict that pathways leading to decreased CBP/p300 levels might sensitize cells to stimuli promoting apoptosis, cell proliferation or differentiation.

We undertook this study to explore the relation of CBP and p300 proteins with continuous mitogenic stimuli and the putative signaling mechanisms controlling these HAT proteins, including the Ras pathway.

MATERIALS AND METHODS

Cell lines, transfections, and antibodies

NIH3T3 fibroblasts, CV1 and CV1COS cell lines were maintained in Dulbecco's modified Eagle's medium (DMEM; Invitrogen, Carlsbad, CA) supplemented with 10 % calf serum (CS, Invitrogen). Stable transfections were done using the calcium phosphate precipitation technique (20, 27). Transfected cell lines were also selected in medium supplemented, as appropriate, with Geneticin 750 $\mu\text{g/ml}$ (Invitrogen). Transient transfections were performed with the Lipofectamine reagent (Invitrogen). Transfected cells were washed after 14 h and harvested 36 h after transfection. Finally, they were washed once in phosphate-buffered saline (PBS). Proteasome inhibition was achieved by treatment with MG132 or ALLN (Sigma). PDGF and the monoclonal antibodies anti-tubulin and anti-Flag were purchased from Sigma Aldrich (St Louis, MO). Monoclonal antibodies to phospho-MAPK (p-ERK1/p-ERK2) and phospho-AKT proteins were purchased from New England Biolabs (Beverly, MA). Rabbit polyclonal antiserum to MAPK (ERK1/ERK2), anti-CBP (A-22, raised against a peptide not conserved on p300; mapping at the amino terminus of human CBP; does not cross-reacts with p300), anti-p300 (C-20, raised against C-terminus of human p300; does not cross-reacts with CBP) anti-Mdm2, anti-poly-ubiquitin and anti-AKT were obtained from Santa Cruz Biotechnology Inc. (Santa Cruz, CA); anti-Ral monoclonal antibody was purchased from Transduction Laboratories (Lexington, KY); and anti-HA and anti-AU5 monoclonal antibodies from the Berkeley Antibody Company (Berkeley, CA).

DNA constructs

The plasmids pCEFL-KZ-AU5, pCEFL-KZ-AU5-H-Ras V12, pCEFL-KZ-AU5-K-Ras V12 and pCEFL-KZ-AU5-N-Ras V12, were previously described (20, 27). pCDNA3-HA-CBP has been described elsewhere (4, 9). pCDNA3-GAGA and pCDNA3-Flag-p300 were kind gifts from Drs. J. Bernués and S. Pons respectively. pCDNA3-CBP (ΔMdm2) (1098-2441) was a kind gift from Dr. L. Vandel. PXJ-Mdm2 (expressing mouse Mdm2) and pXJ Mdm2 C462A were kind gifts from Dr. B. Wasylyk and Dr. D. Trouche (28). pCMV-Collagenase-luciferase and pCDNA3-HA-Ubiquitin were kind gifts from Dr. C. Caelles and Dr T. Thonson respectively.

Cell extract preparation

Total cell extracts were prepared in IPH buffer (4) by keeping the cells on ice for 20 min followed by centrifugation at 13.000 rpm for 10 min at 4° C. All buffers contained protease inhibitors (Boehringer). Analysis of steady-state levels for CBP and p300 were conducted as follows: for endogenous CBP/p300, NIH3T3 fibroblasts were lysed directly by boiling in Laemmli sample buffer, or extracted using IPH buffer as indicated above; for transfected CBP/p300, cells were lysed in 100µl of luciferase lysis buffer (Promega). Luciferase activity was measured according to the manufacturer's instructions. Fifty µl of 4x Laemmli sample buffer were then added to the cells to prepare the total cell lysates. After boiling and centrifugation, a defined amount of lysate (according to the luciferase activity) was collected and then adjusted to 25 µl with 1x Laemmli sample buffer, before being subjected to immunoblot analysis.

Cell proliferation assays.

The measurement of doubling time and saturation density was carried out by a modification of a previously described method (11). NIH3T3 transfectants were seeded at a density of 4×10^4 cells/60 mm plate in CS (10%)-containing DMEM. Cells were counted 24 h later; this time point was considered day 0. The remaining cultures were incubated either in low (0.5%) or high (10%) serum-containing DMEM and replenished every 2 days. Cells were trypsinized and counted by a hemocytometer every 2 days. Some of the cells grown under high serum conditions were allowed to reach confluence and were counted 8 days later.

Bacterial expression of fusion proteins

The plasmid pGEX-Ral-BD containing the Ral A-binding domain fused to glutathione S-transferase (GST) were kindly provided by J.L. Bos. All GST-fusion proteins were purified (from *E. coli* BL21 (DE3) harboring these plasmids) following the method previously described (20).

Pull-down assays

Transfected cells were lysed in cold lysis buffer containing 25mM HEPES pH 7.5, 1% NP-40, 0.25% Na-deoxycholate, 10% glycerol, 1 mM EDTA, 150 mM NaCl, 10mM

MgCl₂, 1mM sodium orthovanadate (Na₃VO₄), 25mM NaF, 1mM PMSF, 10µg/ml of leupeptin, aprotinin, pepstatin A and trypsin inhibitor. Nucleus-free supernatants were incubated with GST-Ral-BD on glutathione-sepharose beads and analyzed as previously described (20).

HAT assays

In vitro acetylation assays were performed as previously described (29).

Immunoprecipitation and immunoblot analyses

Immunoprecipitation and immunoblot analyses were performed as described elsewhere (20). Quantifications from immunoblots were performed using Gene Tools from the Syngene programme.

RT-Quantitative Real-Time-PCR

Total cellular RNA extracts were obtained using Ultraspec Rna Isolation System (Biotecx); subsequently, total RNA was passed to cDNA with the Omniscript Reverse Transcription kit (Qiagen). Differences in the RNA content from the four cell lines were determined by real-time PCR using the ABI 7700 Sequence Detection System and SYBR Green Master Mix protocol (Applied Biosystems). PCR reactions were carried out in triplicate using fixed amounts of template DNA from each cell line at 95°C for 10 min, followed by 40 cycles of 15 s at 95°C and 1 min at 60°C. A standard curve was made for each amplicon by plotting the number of cycles at which the fluorescence crossed the threshold (crossing values) against increasing amounts of DNA template. All PCR products were approximately 50 bp long to increase the efficiency of real-time reactions. All experimental values were normalized to those obtained for tubulin.

Immunocytochemistry

Cells on cover slips were fixed in 4% p-formaldehyde in PBS for 30 min at room temperature and permeabilized with methanol for 10 min. After blocking with 3% BSA in PBS, 0,1% Tween 20 for 1 h at room temperature, cover slips were incubated with a 1:200 anti HA antibody in PBS, 3% BSA for 2h, followed by incubation for 1 h with Cy3-conjugated goat anti-mouse IgG, used at 1:250 dilution in PBS, 3% BSA. After

every incubation with the antibody, cover slips were thoroughly washed with PBS, 0,05% Tween 20 four times for 10 min each at room temperature. The nuclei were stained with DAPI.

Reporter gene analysis

NIH3T3 cells and Ras V12 overexpressing cell lines were transfected with 2 µg of pCMV-Collagenase-luciferase, 1µg of TK-*Renilla* in the presence or absence of pCDNA3-HA-CBP or pCDNA3-Flag-p300. Whole cell extracts were used in the luciferase and *Renilla* assays.

RNA interference

Target sequences for small interfering RNAs for Mdm2 are as follows: sense sequences 5'-GGUUAUAUGACGAGAAGCAtt- 3'; 5'-GGAGCACAGGAAAUAUAUtt- 3'; 5'-GGACUUUGGAAGUGUAUGUtt- 3'; Mdm2 and non-specific control were synthesized by Ambion. The siRNAs were transfected twice using Jet-Pei™ (Polyplus-Transfection, Illkirch, France) at 24-h intervals.

RESULTS

CBP/p300 HAT activity and protein levels specifically decrease in NIH3T3 fibroblasts overexpressing hyperactive Ras

We analyzed the CBP and p300 proteins levels in NIH3T3 fibroblasts at different times upon PDGF-Receptor stimulation, by immunoblot analysis using antibodies that specifically recognize either CBP or p300. In agreement with previous data (30, 31), this mitogenic stimulus induced ERK and AKT activation (Fig 1A). However, we also detected a significant decreased (60-80%) of CBP and p300 levels (Fig 1B). Since ERK and AKT are activated by signaling pathways downstream Ras, we analyzed CBP/p300 co-activators following Ras activation. To this end, we used as model NIH3T3 cell lines stably transfected with either H-Ras, N-Ras or K-Ras4B mutated at position 12, Ras V12 (which causes Ras proteins to become constitutively active) (20). These transfectant cell lines displayed transforming activity (Fig 2) characterized by: morphological alterations; disruption of actin stress fibers with high numbers of membrane ruffles and lamellipodia (20); cell growth alterations with significantly shorter doubling times and higher saturation densities than NIH3T3 cells transfected only with the vector (control cells) (Fig 2A); and activation of the different Ras-dependent pathways (Fig 2B). We found a sharp decrease of CBP and p300 protein levels after H-Ras V12 and N-Ras V12 overexpression and a slight decrease after K-Ras4B V12 overexpression (Fig 3A, left panel). The CBP and p300 proteins were not absent from the H and N-Ras V12-transformed cell extracts, since longer exposure allows the detection of both CBP and p300 (Fig 3A, right panel). In contrast to the observed drop of CBP/p300 levels, neither TAF II p250, P/CAF nor HDAC1 levels changed upon Ras-V12 (H, N or K-Ras4B) overexpression (data not shown). To confirm that the decrease in CBP/p300 levels is not only consequence of differences in cell proliferation, we have analyzed the CBP/p300 levels in CV1 and CV1 T antigen transformed (CV1COS) cell lines. T antigen induces proliferation mainly by inactivating pRb; this inactivation results in an activation of E2F-regulated genes that leads to cell proliferation (32). We find (Figure 3B) that both CV1 T transformed and non-transformed cells have similar CBP/p300 levels. This points to Ras pathway activation as a responsible for the CBP/p300 observed decrease. According to these

results, CBP and p300 HAT activities also decreased (by 50-80%) following Ras V12-overexpression (Fig 3C). The CBP/p300 HAT activity is similar for the H, K and N-Ras V12, however, the CBP/p300 levels are higher in the case of K-Ras V12, suggesting the existence of an additional negative regulation of CBP/p300 HAT activity by K-Ras V12 as have been already proposed by other oncogenic proteins (33, 34) (See also figure 3D).

To investigate whether Ras V12 expression inhibit not only CBP/p300 HAT activity, but also CBP/p300 induced-transcriptional activity, NIH3T3 and Ras-overexpressing cell lines were transiently transfected with Collagenase-luciferase vector (which is coactivated by CBP/p300) and the transcriptional activity of this promoter was analyzed in the presence or absence of overexpressed CBP/p300. Figure 3D shows that CBP coactivates the collagenase promoter the in NIH3T3 control cells, however this effect is very reduced in Ras V12 overexpressing cell lines. To confirm these results, we have analyzed the effects of Ras pathway activation on the expression of an endogenous target gene, the transglutaminase gene (TGase). It has been previously shown (35) that EGF represses the RA-mediated induction of TGase gene in NIH3T3 cells; then, we have decided to asses whether RA is still able to induce TGase gene in H-Ras V12 overexpressing cell line. Real-time experiments in figure 3E show that after RA treatment the TGase RNA levels increase in NIH3T3 control cells, but not in H-Ras V12 overexpressing cells. Taken together, these results demonstrate a specific loss of CBP and p300 following overexpression of hyperactive Ras on NIH3T3 cells, resulting in a drop of their transcriptional and HAT activities.

CBP/p300 is degraded through the ubiquitin-proteasome pathway in NIH3T3 fibroblasts overexpressing Ras V12

We investigated the possible causes of CBP/p300 loss. Real time RT-PCR analysis was performed, and the results revealed that CBP and p300 RNA levels were slightly lower in Ras-overexpressing cells than in control cells, mainly in the case of K-Ras V12 (Fig 4A). However, this decrease was not as dramatic as was the CBP and p300 drop-off in protein levels, particularly in the case of H-Ras V12 and N-Ras V12, suggesting that the reduction in CBP/p300 protein levels could be due to an additional mechanism(s), most likely proteolytic processing. We therefore tested different protease

inhibitors for their ability to reverse CBP and p300 degradation. The proteasome inhibitor ALLN reversed the CBP/p300 decrease observed by H-Ras V12, K-Ras V12, and N-Ras V12 overexpression (Fig 4B). Similar results were obtained after treating the cells with MG132, another proteasome inhibitor (data not shown). These results suggested that CBP/p300 may be degraded by the proteasome pathway in Ras V12-overexpressing NIH3T3 fibroblasts. To confirm these results, we investigated whether the CBP/p300 half-life was shorter in Ras V12-overexpressing cells than in NIH3T3 control cells. Unfortunately, we could not consistently detect endogenous CBP/p300 in the absence of proteasome inhibitors (see e.g. Fig 3A, lanes 2 and 4). As the decrease of CBP/p300 levels was more dramatic for H-Ras V12 and N-Ras V12, we focused on the NIH3T3 cells overexpressing these proteins to analyze the molecular mechanisms involved in the effects on CBP/p300.

We therefore tested whether CBP/p300 is ubiquitinated in these cells. To this end, NIH3T3 cells were transfected with HA-ubiquitin and Flag-p300 expression vectors in the presence or absence of H-Ras V12. HA-ubiquitinated proteins were immunoprecipitated, and the amount of ubiquitinated Flag-p300 was determined by immunoblotting using anti-Flag antibody. The level of p300 poly-ubiquitination increased, and some new bands appeared following H-Ras V12 overexpression (Fig 4C), suggesting that p300 is degraded in these cells through the ubiquitin-proteasome system.

Mdm2 induces degradation of CBP/p300

Since Mdm2 is responsible for the degradation of several HATs (TIP 60, P/CAF) (36, 37), and inhibits CBP/p300-mediated p53 acetylation by its interaction with these two proteins (38-40), we hypothesized that Mdm2 could be responsible for CBP/p300 degradation in NIH3T3 cells overexpressing Ras V12. To test this hypothesis, we transfected NIH3T3 cells with Flag-tagged p300 expression plasmid, TK-luciferase reporter, and GAGA expression plasmid as an internal control, either in the presence or in the absence of Mdm2 and H-Ras V12 expressing vectors. After standardization using luciferase activity for transfection efficiency we analyzed total extracts for the expression levels of p300, Mdm2 and GAGA proteins by immunoblotting with antibodies against Flag, Mdm2 and GAGA, respectively. Co-

expression of H-Ras V12 and Mdm2 led to a significant reduction in Flag-p300 levels (Fig 5A lane 4), whereas the amount of GAGA remained unaffected. To confirm these results we analyzed the CBP and p300 degradation induced by an Mdm2 mutated (C462A) in the RING-finger domain without any ubiquitin ligase activity. The results showed that Mdm2 wt induced a sharp decrease of CBP and p300 levels, whereas in the case of mutant Mdm2 C462A the effects were significantly reduced (Fig 5B compare lanes 2 and 3). Same results were obtained for N-Ras V12 (data not shown).

CBP and Mdm2 interact through the N-terminal domain of CBP (38). To investigate whether CBP degradation requires the CBP-Mdm2 interaction domain, we analyzed the HA-CBP full-length (FL) and HA-CBP deletion mutant (Δ Mdm2, which lacks the Mdm2 interacting region) protein levels in NIH3T3 control cells as well as in H-Ras V12 or N-Ras V12 overexpressing cells. Our results demonstrated that both proteins CBP (FL) and CBP (Δ Mdm2) were easily revealed by indirect immunostaining with anti-HA antibody in NIH3T3 control cells (Fig 6A). However, only the CBP (Δ Mdm2) mutant was clearly detected in all transfected Ras V12-overexpressing cells, whereas CBP (FL) was only visible in a small number of these cells (35-43% of transfected cells, Fig 6A).

To confirm these results we knock-down Mdm2 expression in NIH3T3 H-Ras V12 cells using small interfering RNAs (siRNAs). These cells were transfected with siRNA pool control, or with siRNA pool covering different portions of the mouse Mdm2 coding sequence. Endogenous Mdm2 was decreased by 40-60% using this siRNA pool (Fig 6B). Under these conditions the endogenous levels of tubulin were not affected. However, decreased Mdm2 expression correlated with an increase of the CBP and p300 protein levels (Fig 6B), suggesting that in NIH3T3 H-Ras V12 cell lines Mdm2 contributes to degrade CBP and p300. Since our data indicated that Mdm2 may be involved in CBP/p300 loss in Ras V12-transformed fibroblasts, we tried to assess whether these cell lines exhibited increased levels of Mdm2 protein relative to NIH3T3 control cells. Consistent with the above proposed role of Mdm2 in CBP/p300 degradation, we found that Mdm2 levels increased in NIH3T3 fibroblasts overexpressing also Ras V12 (Fig 6C), as shown previously by others (15).

DISCUSSION

The findings presented in this report show that CBP/p300 is regulated by proteasome-mediated proteolysis in Ras V12-overexpressing NIH3T3 cells. We found that Mdm2 induces CBP/p300 degradation in the presence of Ras active proteins. These data also show that CBP/p300 themselves are direct targets for MAPK signaling pathway as have been previously suggested by others (13, 41-43).

The observation that Ras pathway activation and CBP/p300 degradation are associated might appear paradoxical. On the one hand, many genes involved in cellular proliferation require CBP/p300 as a coactivators. In fact several reports support this idea showing CBP/p300 activation via MAPK cascade (41-45). On the other hand, many studies have shown that CBP/p300 family members possess tumor suppressor-like function. Mice heterozygous for CBP have an increased rate of malignancies than wild-type mice (24); human patients with Rubinstein-Taybi syndrome, due to CBP heterozygosity, also show an increased rate of malignancies (46). Very recently it has been shown that suppression of the activated Ras phenotype occurs by two point mutations in the *C. elegans* p300/CBP homolog, *cbp-1*. One of these mutations results in an increase of HAT *cbp-1* activity, suggesting a role for *cbp-1* as a negative regulator of Ras signaling (47). In the same line of evidence Poizat and colleagues (48) have shown that activation of the p38 MAPK pathway by doxorubicin and degradation of p300 are coupled. The paradox might be explained by the different effects of Ras activation depending on the cellular environment: Ras activation leads to senescence induction; when another genetic alteration occurs oncogenic Ras may cause transformation. It is possible that oncogenic Ras may induce senescence only in some cell types or together with other signals. In fact Deng and colleagues (49) have shown that p300/CBP play a critical role in the Ras-triggered senescence and inactivation of these coactivators in conjunction with other genetic alterations can contribute to Ras-induced transformation and tumorigenesis. Then, CBP/p300 play a critical role limiting the oncogenic potential of Ras.

We have detected that continuous mitogenic stimulation induces loss of CBP and p300 in NIH3T3 fibroblasts, and these effects can be reproduced by overexpression

of Ras V12. The loss of CBP and p300 proteins is probably the main cause of the CBP/p300 HAT-activity decrease observed after H-Ras V12 and N-Ras V12 overexpression. However, in the case of K-Ras4B V12 an additional negative regulation of CBP/p300 HAT activity probably occurred, as has been described in other oncoproteins (33, 34). Interestingly, our data suggest that the levels of CBP/p300 proteins were different according to the type of Ras V12-overexpressing cells analyzed. Therefore, during H- and N-Ras (V12) overexpression, a sharp reduction of CBP/p300 protein levels was observed, particularly in the latter. Furthermore, in the case of K-Ras V12 a clear effect on CBP/p300 RNA levels was observed (currently under study in our laboratory) (Fig 4A), whereas for H and N-Ras (V12) overexpression the main contribution to the decrease of CBP/p300 levels was protein degradation. Although there is high degree of sequence homology between Ras proteins, accumulating evidence supports the idea of different roles for the three Ras homologues (15, 18), as was suggested by the embryonic lethality observed in the *Kras*, but not in the *Hras* or *Nras*, knockout mice (21). Moreover, N-Ras and H-Ras proteins can be reversibly palmitoylated at one or two cysteine residues, respectively, while K-Ras possesses a polybasic domain close to the C-terminal end, variations which may contribute to differences in trafficking (50), membrane association, and effector pathway engagement between the three Ras homologues (51). Indeed, it has been recently demonstrated that the activation of H-Ras and N-Ras proteins (but not K-Ras) in the Golgi apparatus and in the endoplasmic reticulum (52, 53) depends upon Ras-GRP and Ras-GRF proteins, respectively (54, 55). The functional specificity in signaling by the three homologues is also apparent in the differences in the relative ability of H-Ras versus K-Ras to activate the Raf and PI3K effector pathways (56). Indeed, it has been suggested that K-Ras activates Rac more efficiently than H-Ras (57), or that H-Ras and K-Ras induce higher activation of NF- κ B than N-Ras (58). As these data support the idea that the Ras proteins (H-, K-, and N-Ras) have distinct behaviors *in vivo*, the different effects on CBP/p300 levels could be other more phenotypic manifestation of this dissimilar role, as occurs with the differing presence of oncogenic *ras* in human tumors (15).

CBP/p300 are components of the transcription machinery and integrate multiples signals to regulate gene expression in response to different signals. CBP/p300 are able to mediate the expression of genes implicated in many responses, such as proliferation,

cell cycle arrest, differentiation, transformation, etc, depending on the extra and intracellular signals. Regulation of CBP/p300 might be then critical to mediate specific transcriptional responses. Since there are a large number of signal transduction pathways requiring the activity of CBP/p300 co-activators, the availability of these proteins is a critical step in many biological processes. In fact, a direct antagonism between promoters that require CBP/p300 as co-activators has been previously described (14, 59). In particular, it is known that agonists of the Ras pathway promote the interaction of CBP with the MAP kinase p90RSK, which thereby inhibits the activation of CREB-responsive elements by cAMP (60). Therefore, the alterations in CBP/p300 levels that we have described here following Ras-overexpression in NIH3T3 cells may interfere with other signal transduction pathways through competition for limiting concentration of CBP/p300, thus altering their specificity for selected promoters.

In accordance with the present data, it would be very interesting to determine whether responses to other signaling pathways are affected in Ras V12-overexpressing NIH3T3 cells in a CBP/p300-dependent manner, and the putative relation between loss of CBP/p300 protein levels and the transforming effects mediated by hyperactive Ras. Moreover, it would also be helpful to examine whether CBP/p300 are similarly targeted by the proteasome degradation pathway in human tumors induced by Ras oncogenes.

ACKNOWLEDGEMENTS

We would like to thank Dr. L. Vandel for constructs and for critical reading of the paper. Dr. X. de la Cruz for suggestions and for critical review of the paper. Dr B. Piña for suggestions and technical support with the Real-Time-PCR and Drs. D. Trouche, B. Wasylyk, J. Bernués, J.L. Bos, C. Caelles, S. Pons and T. Thonson for constructs. This work was supported by grants to MMB from the Ministerio de Educación y Ciencia, SAF2002-00741 and PAMNBMB; and to JMR, SAF2003-02604. SSM is the recipient of a fellowship from the Generalitat de Catalunya.

REFERENCES

1. Hebbes, T.R., Thorne, A.W. and Crane-Robinson, C. (1988) A direct link between core histone acetylation and transcriptional activite chromatin. *EMBO J.* **7**, 1395-1402
2. Sterner, D.E. and Berger, S.L. (2000) Acetylation of histones and transcription-related factors. *Microbiol. Mol. Biol. Rev.* **64**, 435-459
3. Ogryzko, V.V., Schiltz, R.L., Russanova, V., Howard, B.H. and Nakatani, T. (1996) The transcriptional co-activators p300 and CBP are histone acetyltransferases. *Cell* **87**, 1107-1112
4. Bannister, A.J. and Kouzarides, T. (1996) The CBP co-activator is a histone acetyltransferase. *Nature* **384**, 641-643
5. Gu, W. and Roeder, R.G. (1997) Activation of p53 sequence-specific DNA binding by acetylation of p53 C-terminal domain. *Cell* **90**, 595-606
6. Imhof, A., Yang, X.J., Ogryzko, V.V., Nakatani, Y., Wolfe, A.P. and Ge, H. (1997) Acetylation of general transcription factors by histone acetyltransferases. *Curr. Biol.* **7**, 689-692
7. Boyes, J., Byfield, P., Nakatani, Y. and Ogryzko, V. (1998) Regulation of activity of the transcription factor GATA-1 by acetylation. *Nature* **396**, 594-598
8. Martínez-Balbás, M.,A. Bauer, U-M, Nielsen, S.J., Brehm, A. and Kouzarides, T. (2000) Regulation of E2F1 activity by acetylation. *EMBO J.* **19**, 662-671
9. Santos-Rosa, H., Valls, E., Kouzarides, T. and Martínez-Balbás, M.A. (2003) Mechanisms of P/CAF auto-acetylation. *Nucleic Acids Res.* **31**, 4285-4292

10. Bayle, J.H. and Crabtree, G.R. (1997) Protein acetylation: more than chromatin modification to regulate transcription. *Chem. Bio.* **4**, 885-888
11. Chan, H.M. and La Thangue, N.B. (2001) p300/CBP proteins: HATs for transcriptional bridges and scaffolds. *J. Cell. Sci.* **114**, 2363-2373
12. Vo, N. and Goodman, R.H. (2001) CREB-binding protein and p300 in transcriptional regulation. *J. Biol. Chem.* **276**, 13505-13508
13. Goodman, R.H. and Smolik, S. (2000) CBP/p300 in cell growth, transformation, and development. *Genes & Dev.* **14**, 1553-1577
14. Kamei, Y., Xu, L., Heinzel, T., Torchia, J., Kurokawa, R., Glass, B., Lin, S.C., Heyman, R.A., Rose, D.W., Glass, C.K. and Rosenfeld, M.G. (1996) A CBP integrator complex mediates transcriptional activation and AP-1 inhibition by nuclear receptors. *Cell* **85**, 403-414
15. Rojas, J.M. and Santos, E. (2002) The ras genes and human cancer: different implications and different roles. *Current Genomics* **3**, 295-311
16. Wittinghofer, A. and Nassar, N. (1996) How Ras-related proteins talk to their effectors. *Trends Biochem. Sci.* **21**, 488-491
17. Rommel, C. and Hafen, E. (1998) Ras-a versatile cellular switch. *Curr. Opin. Genet. Dev.* **4**, 412-418
18. Shields, J.M., Pruitt, K., McFall, A., Shaub, A. and Der, C.J. (2000) Understanding Ras: 'it ain't over 'til it's over'. *Trends Cell. Biol.* **4**, 147-154
19. Oliva, J.L., Perez-Sala, D., Castrillo, A., Martinez, N., Canada, F.J., Bosca, L. and Rojas, J.M. (2003) The cyclopentenone 15-deoxy-delta 12,14-prostaglandin J2 binds to and activates H-Ras. *Proc. Natl. Acad. Sci. U S A* **100**, 4772-4777

20. Oliva, J.L., Zarich, N., Martinez, N., Jorge, R., Castrillo, A., Azanedo, M., Garcia-Vargas, S., Gutierrez-Eisman, S., Juarranz, A., Bosca, L., Gutkind, J.S. and Rojas, J.M. (2004) The P34G mutation reduces the transforming activity of K-Ras and N-Ras in NIH 3T3 cells but not of H-Ras. *J. Biol. Chem.* **279**, 33480-33491
21. Esteban, L.M., Vicario-Abejon, C., Fernandez-Salguero, P., Fernandez-Medarde, A., Swaminathan, N., Yienger, K., Lopez, E., Malumbres, M., McKay, R., Ward, J.M., Pellicer, A. and Santos, E. (2001) Targeted genomic disruption of H-ras and N-ras, individually or in combination, reveals the dispensability of both loci for mouse growth and development. *Mol. Cell. Biol.* **5**, 1444-1452
22. Giles, R.H., Peters, D.J.M. and Breuning, M.H. (1998) Conjunction dysfunction: CBP/p300 in human disease. *Trends Genet.* **14**, 178-183
23. Gayther, S.A., Batley, S.J., Linger, L., Bannister, A., Thorpe, K., Chin, S., Daigo, Y., Russell, P., Wilson, A., Sowter, H.M., Delhanty, J.D., Ponder, B.A., Kouzarides, T. and Caldas, C. (2000) Mutations truncating the EP300 acetylase in human cancers. *Nat. Genet.* **24**, 300-304
24. Kung, A.L., Rebel, V.I., Bronson, R.T., CH'ng, L., Sieff, C.A., Livingsgton, D.M. and Yao, T. (2000) Gene dosage-dependent control of hematopoiesis and hematologic tumor suppression by CBP. *Genes & Dev.* **14**, 272-277
25. Petrij, F., Giles, R.H., Dauwerse, H.G., Saris, J.J., Hennekam, R.C., Masuno, M., Tommerup, N., van Ommen, G.J., Goodman, R.H. and Peters D.J. (1995) Rubinstein-Taybi syndrome caused by mutations in the transcriptional co-activator CBP. *Nature* **376**, 348-351
26. Alarcon, J.M., Malleret, G., Touzani, K., Vronskaya, S., Ishii, S., Kandel, E.R. and Barco, A. (2004) Chromatin acetylation, memory, and LTP are impaired in

CBP^{+/-} mice: a model for the cognitive deficit in Rubinstein-Taybi syndrome and its amelioration. *Neuron* **42**, 947-959

27. Jorge, R., Zarich, N., Oliva, J.L., Azanedo, M., Martinez, N., de la Cruz, X. and Rojas, J.M. (2002) HSos1 contains a new amino-terminal regulatory motif with specific binding affinity for its pleckstrin homology domain. *J. Biol. Chem.* **46**, 44171-44179

28. Argentini, M., Barboule, N. and Wasyluk, B. (2000) The contribution of the RING finger domain of MDM2 to cell cycle progression. *Oncogene* **19**, 3849-3857

29. Martínez-Balbás, M.A., Bannister, A., Martín, K., Haus-Seuffert, P., Meisterernst, M. and Kouzarides, T. (1998) The CBP histone acetyltransferase activity stimulates transcripcion. *EMBO J.* **17**, 2886-2893

30. Gu, J., Tamura, M. and Yamada, K.M. (1998) Tumor suppressor PTEN inhibits integrin- and growth factor-mediated mitogen-activated protein (MAP) kinase signaling pathways. *J Cell Biol.* **143**, 1375-83

31. Soskic, V., Gorlach, M., Poznanovic, S., Boehmer, F.D. and Godovac-Zimmermann, J. (1999) Functional proteomics analysis of signal transduction pathways of the platelet-derived growth factor beta receptor. *Biochemistry* **38**, 1757-1764

32. Moran, E. (1993) DNA tumor virus transforming proteins and the cell cycle. *Curr. Opin. Gent. Dev.* **3**, 63-70

33. Hamamori, Y., Sartorelli, V., Ogryzko, V., Puri, P.L., Wu, H.Y., Wang, J.Y., Nakatani, Y. and Kedes, L. (1999) Regulation of histone acetyltransferases p300 and PCAF by the bHLH protein twist and adenoviral oncoprotein E1A. *Cell* **59**, 405-413

34. Chakravarti, D., Ogryzko, V., Kao, H.-Y., Nash, A., Chen, H., Nakatani, Y. and Evans, R.M. (1999) A viral mechanism for the inhibition of p300 and P/CAF acetyltransferase activity. *Cell* **96**, 393-403
35. Antonyak, M.A., McNeill, C.J., Wakshlag, J.J., Boehm, J.E. and Cerione, R.A. (2003) Activation of the Ras-ERK pathway inhibits retinoic acid-induced stimulation of tissue transglutaminase expression in NIH3T3 cells. *J. Biol. Chem.* **278**, 15859-15866
36. Legube, Iyer, N.G., Ozdag, H. and Caldas, C. 2004. p300/CBP and cancer. *Oncogen* **24**, 4225-4231
37. Jin, Y., Zeng, S.X., Lee, H. and Lu, H. (2004) MDM2 mediates p300/CREB-binding protein-associated factor ubiquitination and degradation. *J. Biol. Chem.* **279**, 20035-20043
38. Grossman, S.R., Perez, M., Kung, A.L., Joseph, M., Mansur, C., Xiao, Z.-X., Kumar, S., Howley, P.M. and Livingston, D.M. (1998) P300/MDM2 complexes participate in MDM2-mediated p53 degradation. *Mol. Cell* **2**, 405-415
39. Kobet, E., Zeng, X., Zhu, Y., Keller, D. and Lu, H. (2000) MDM2 inhibits p300-mediated p53 acetylation and activation by forming a ternary complex with the two proteins. *Proc. Natl. Acad. Sci. U S A* **97**, 12547-12552
40. Ito, A., Lai, C.H., Zhao, X., Saito, S., Hamilton, M.H., Paella, E. and Yao, T.P. (2001) p300/CBP-mediated p53 acetylation is commonly induced by p53-activating agents and inhibited by MDM2. *EMBO J.* **20**, 1331-134041
41. Gusterson, R., Brar, B., Faulkes, D., Giordano, A., Chrivia, J. and Latchman, D. (2002) The transcriptional co-activators CBP and p300 are activated via phenylephrine through the p42/p44 MAPK cascade. *J. Biol. Chem.* **277**, 2517-2524

42. Li QJ, Yang SH, Maeda, Y., Sladek, F.M., Sharrocks, A. and, Martins-Green, M. (2003) MAP kinase phosphorylation-dependent activation of Elk-1 leads to activation of the co-activator p300. *EMBO J.* **22**, 281-291
43. Ait-Si-Ali, S., Carlisi, D., Ramirez, S., Upegui-Gonzalez, L.C., Duquet, A., Robin, P., Rudkin, B., Harel-Bellan, A. and Trouche, D. (1999) Phosphorylation by p44 MAP Kinase/ERK1 stimulates CBP histone acetyl transferase activity in vitro. *Biochem. Biophys. Res. Commun.* **262**, 157-162
44. Gusterson, R.J., Yuan, L.W. and Latchman, D.S. (2004) Distinct serine residues in CBP and p300 are necessary for their activation by phenylephrine. *Int. J. Biochem. Cell. Biol.* **36**, 893-899
45. Liu, Y.Z., Chrivia, J.C. and Latchman, D.S. (1998) Nerve growth factor up-regulates the transcriptional activity of CBP through activation of the p42/p44(MAPK) cascade. *J. Biol. Chem.* **273**, 32400-32407
46. Miller, R.W. and Rubinstein, J.H. (1995) Tumors in Rubinstein-Taybi syndrome. *Am. J. Med. Genet.* **56**, 112-115
47. Eastburn, D.J. and Han, M. (2005) A gain-of-function allele of *cbp-1*, the *Caenorhabditis elegans* ortholog of the mammalian CBP/p300 gene, causes an increase in histone acetyltransferase activity and antagonism of activated Ras. *Mol. Cell. Biol.* **25**, 9427-9434
48. Poizat, C, Puri, P.L., Bai, Y. and Kedes, L. (2005) Phosphorylation-dependent degradation of p300 by doxorubicin-activated p38 mitogen-activated protein kinase in cardiac cells. *Mol. Cell. Biol.* **25**, 2673-2687
49. Deng, Q., Li, Y., Tedesco, D., Liao, R., Fuhrmann, G. and Sun, P. (2005) The ability of E1A to rescue ras-induced premature senescence and confer

transformation relies on inactivation of both p300/CBP and Rb family proteins. *Cancer Res.* **65**, 8298-8307

50. Apolloni, A., Prior, I.A., Lindsay, M., Parton, R.G. and Hancock, J.F. (2000) H-ras but not K-ras traffics to the plasma membrane through the exocytic pathway. *Mol. Cell. Biol.* **20**, 2475-2487

51. Matallanas, D., Arozarena, I., Berciano, M.T., Aaronson, D.S., Pellicer, A., Lafarga, M. and Crespo, P. (2003) Differences on the inhibitory specificities of H-Ras, K-Ras, and N-Ras (N17) dominant negative mutants are related to their membrane microlocalization. *J. Biol. Chem.* **278**, 4572-4581

52. Chiu, V.K., Bivona, T., Hach, A., Sajous, J.B., Silletti, J., Wiener, H., Johnson, R.L. 2nd, Cox, A.D. and Philips, M.R. (2002) Ras signalling on the endoplasmic reticulum and the Golgi. *Nat. Cell Biol.* **4**, 343-350

53. Roy, S., Wyse, B. and Hancock, J.H. (2002) H-Ras Signaling and K-Ras Signaling Are Differentially Dependent on Endocytosis. *Mol. Cell. Biol.* **22**, 5128-5140

54. Caloca, M.J., Zugaza, J.L. and Bustelo, X.R. (2003) Exchange factors of the RasGRP family mediate Ras activation in the Golgi. *J. Biol. Chem.* **278**, 33465-33473

55. Arozarena, I., Matallanas, D., Berciano, M.T., Sanz-Moreno, V., Calvo, F., Munoz, M.T., Egea, G., Lafarga, M. and Crespo, P. (2004) Activation of H-Ras in the endoplasmic reticulum by the RasGRF family guanine nucleotide exchange factors. *Mol. Cell. Biol.* **24**, 1516-1530

56. Yan, J., Roy, S., Apolloni, A., Lane, A. and Hancock, J.F. (1998) Ras isoforms vary in their ability to activate Raf-1 and phosphoinositide 3-kinase. *J. Biol. Chem.* **273**, 24052-24056

57. Walsh, A.B. and Bar-Sagi, D. (2001) Differential activation of the Rac pathway by Ha-Ras and K-Ras. *J. Biol. Chem.* **276**, 15609-15615
58. Millan, O., Ballester, A., Castrillo, A., Oliva, J.L., Traves, P.G., Rojas, J.M. and Bosca, L. (2003) H-Ras-specific activation of NF-kappaB protects NIH 3T3 cells against stimulus-dependent apoptosis. *Oncogene* **22**, 477-483
59. Avantaggiati, M.L., Ogryzko, V., Gardner, K., Giordano, A., Levine, A.S. and Kelly, K. (1997) Recruitment of p300/CBP in p53-dependent signal pathways. *Cell* **89**,1175-1184
60. Nakajima, T., Fukamizu, A., Takahashi, J., Gage, F.H., Fisher, T., Blenis, J. and Montminy, M.R. (1996) The signal dependent coactivator CBP is a nuclear target for pp90RSK. *Cell* **86**, 465-474

FIGURE LEGENDS**FIGURE 1****PDGF stimulation decreases CBP/p300 levels in NIH3T3 cells**

NIH3T3 fibroblasts were stimulated with PDGF (1 mg/ml) for 0, 15 (15'), 30 (30'), 60 (60') min, 1 day (1d), 2 days (2d) to 3 days (3d). Total cell extracts cells were prepared, the total protein amount was adjusted and analyzed as (A) and (B). (A) The ERK (p42 and p44 proteins) and AKT phosphorylation levels were determined using specific anti-phospho- and full antibodies. The fold increase values of p-ERK and p-AKT are the average of three separate assays (in each case with a standard deviation lower than 15% of the average). (B) The CBP and p300 levels were monitored by immunoblot analysis using antibodies against CBP, p300 and tubulin (as an internal control). The diagrams shown relative levels of CBP and p300 after PDGF stimulation of NIH3T3 cells. Histograms correspond to the average and standard deviation of three independent assays.

FIGURE 2**Ras (V12)-expressing cell lines display transforming activity**

(A) Cell doubling times of NIH3T3 clones over-expressing different H, K, or N-Ras (V12) mutants, or transfected only with the vector, were measured as described in the Experimental Procedures section. Doubling time was determined by counting cells every 2 days. Results shown are the mean \pm SD of three independent experiments where each sample was analyzed in triplicate. (B) The expression levels of AU5-Ras (V12) proteins of the above NIH3T3 clones were detected by immunoblotting with monoclonal anti-AU5 (top panel); cell extracts from NIH3T3 fibroblasts transfected with the vector pCEFL-KZ-AU5 (control, C) were included as a negative control. All cells were serum-starved for 18 h and then the ERK (p42 and p44 proteins) and AKT phosphorylation levels were determined using specific anti-phospho- and full antibodies. Ral A-GTP was recovered from cell lysates by binding to immobilized GST-Ral-BD and detected by immunoblotting with the corresponding anti-Ral A monoclonal antibody. The expression levels of the endogenous Ral A protein were detected by immunoblotting of the cell extracts with the corresponding anti-Ral A monoclonal

antibody. Results presented correspond to a representative experiment, and similar results were obtained in three additional, separate experiments.

FIGURE 3

CBP/p300 levels and HAT activity decrease in NIH3T3 fibroblasts overexpressing hyperactive Ras

(A) Total cell extracts from NIH3T3 cells (control cells, C) and NIH3T3 H, K, and N-Ras (V12) overexpressing cells were prepared, the total protein amount was adjusted, and the CBP and p300 levels were monitored by immunoblot analysis using antibodies against CBP, p300 and tubulin (as a loading control). CBP and p300 are not absent from the extract, since longer exposure permit the detection of these proteins. Similar results were obtained when NIH3T3 cells or NIH3T3 Ras overexpressing cells were lysed directly by boiling in Laemmli sample buffer. The results shown are representative of at least six independent experiments. (B) Total cell extracts from CV1 cells and CV1COS (T antigen-expressing cells) were prepared, the total protein amount was adjusted, and the CBP and p300 levels were determined by immunoblotting analysis using antibodies against CBP, p300 and tubulin (as a loading control). (C) Total cell extracts from NIH3T3 cells (control cells, C) and NIH3T3 cells stably transfected with H, K, and N-Ras mutated at position 12 (V12) and AU5 tagged were prepared, the total protein amount was adjusted, and CBP and p300 were immunoprecipitated using antibodies recognizing CBP and p300 proteins and HA protein (as a negative control). The HAT activity associated with the immunoprecipitated proteins was determined in an *in vitro* HAT assay. The average and standard deviations of three independent assays are shown. Immunoblots using antibodies against CBP and p300, performed in parallel to the HAT assay, are shown at the bottom of the figure (D) NIH3T3 and H-RasV12, K-Ras V12 and N-Ras V12 overexpressing cells were transfected with 2 μ g of Collagenase-luciferase reporter, 2 μ g TK-*Renilla* reporter, in the presence or absence of pCDNA3-CBP or pCDNA3-p300 expression vectors. Whole cell extracts were used in the luciferase and *Renilla* assays. The data are an average of at least eight independent transfections. The activity derived from the Collagenase-luciferase reporter was normalized to 1.0 and the other activities are expressed relative to this value. (E) NIH3T3 and H-RasV12 overexpressing cells were treated or not with 5 μ M retinoid

acid (RA) for 2 days in the presence of 1% CS. Total cellular RNA was obtained and the transglutaminase (TGase) RNA content from the two cell lines was determined by real-time PCR using SYBR Green. TGase RNA values were normalized to those obtained for tubulin RNA. The diagrams show the average and standard deviations of two independent experiments performed in triplicate. Immunoblots using antibodies against CBP and tubulin (as a control) of NIH3T3 and H-RasV12 overexpressing cells treated or not with RA are shown at the bottom of the figure.

FIGURE 4

RNA and proteins levels of CBP/p300 decrease in NIH3T3 fibroblasts overexpressing hyperactive Ras

(A) Total cellular RNA from NIH3T3 cells (control cells, C) and NIH3T3 H, K, and N-Ras V12 overexpressing cells was obtained and passed to cDNA. Differences in the RNA content from the four cell lines were determined by real-time PCR using SYBR Green. CBP and p300 RNA values were normalized to those obtained for tubulin RNA. The diagrams show the average and standard deviations of four independent experiments performed in triplicate. (B) Total cell extracts from NIH3T3 cells and NIH3T3 H, K, and N-Ras V12 overexpressing cells treated with ALLN proteasome inhibitor were prepared and the levels of CBP and p300 analyzed by immunoblot. Total protein amounts were loaded into the gels; subsequently immunoblotting was conducted using an antibody against tubulin. (C) Whole-cell extracts from NIH3T3 cells transfected with Flag-p300, HA-ubiquitine and H-Ras V12 expression vectors and treated with MG132 for 12 h were used to immunoprecipitate ubiquitinated proteins, using HA antibody. The immunoprecipitated proteins were analyzed by the presence of poly-ubiquitinated p300 by immunoblotting using an antibody against Flag tag.

FIGURE 5

Mdm2 and Ras V12 co-expression decreases CBP/p300 levels in NIH3T3 cells

(A) NIH3T3 cells were transfected with 100 ng of pCMV luciferase reporter vector, 1 µg of pCDNA3 GAGA, 1 µg of pCDNA3 Flag-p300, in the absence or presence of either 2 µg of pXJ Mdm2 (lanes 3 and 4) or 100 ng of pCEFL-KZ-AU5-H-Ras V12 (lanes 2 and 4). The amount of promoters in the transfection was kept constant by the addition of empty vectors. Luciferase activity was measured 36 h after transfection.

Total cell extracts were prepared and analyzed by immunoblot using specific antibodies directed against Flag (to detect exogenous Flag-p300), Mdm2 and GAGA. (B) NIH3T3 cells were transfected with 100 ng of pCMV luciferase reporter vector, 1 μ g of pCDNA3 GAGA, 1 μ g of pCDNA3 HA-CBP or pCDNA3 Flag-p300 (bottom panel), 100 ng of pCEFL-KZ-AU5-H-Ras V12, in the absence (lane 1) or presence of either 2 μ g of pXJ Mdm2 (lane 2) or 2 μ g of pXJ Mdm2 C462A (lane 3). The amount of promoters in the transfection was kept constant by the addition of empty vectors. Luciferase activity was measured 36 h after transfection. Total cell extracts were prepared and analyzed by immunoblot using specific antibodies directed against HA or Flag (to detect exogenous CBP or p300 respectively), GAGA and Mdm2.

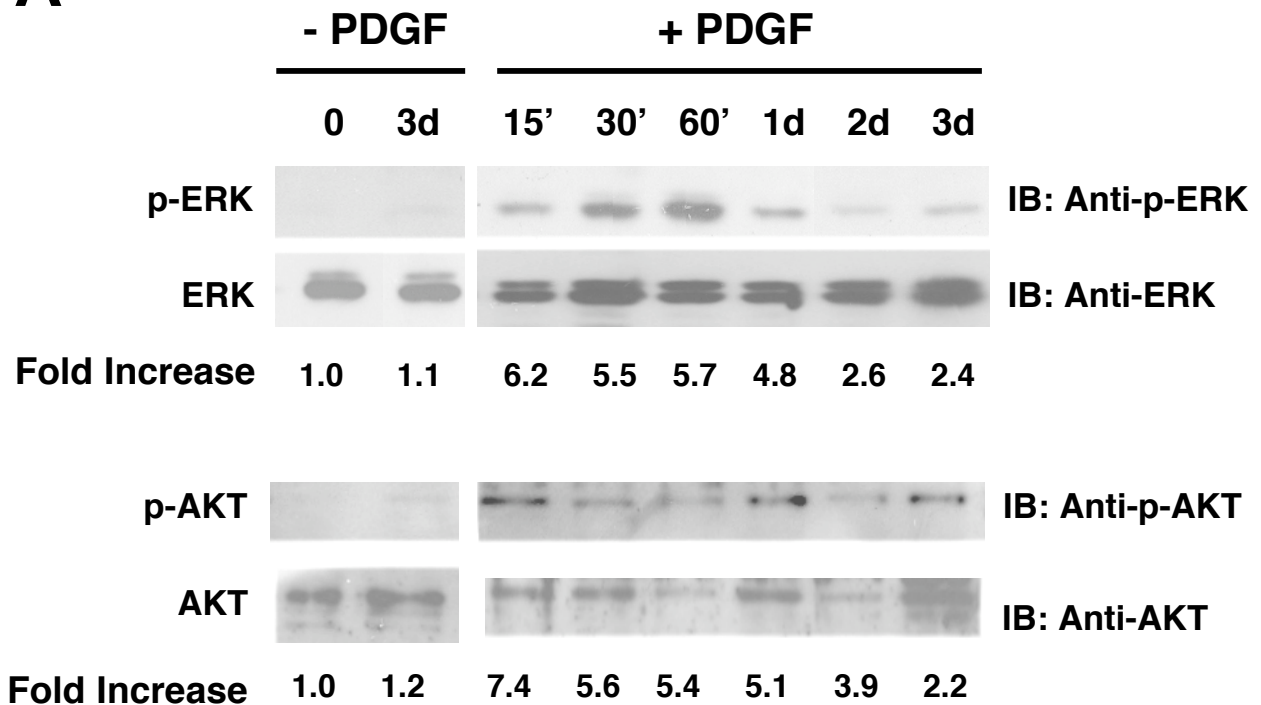
FIGURE 6

Mdm2 decreases CBP/p300 in NIH3T3 fibroblasts overexpressing hyperactive Ras

(A) NIH3T3 cells, NIH3T3 H-Ras V12, and NIH3T3 N-Ras V12 cells lines were transfected with GFP and either pCDNA3 HA-CBP (FL) or pCDNA3 HA-CBP (Δ Mdm2). 36 h after transfection, cells were fixed and HA-CBP was visualized by indirect immunofluorescence using the anti-HA antibody. Transfected cells were detected by the presence of green fluorescence from the GFP protein. Presence of nuclei was followed by DAPI staining. The percentage of transfected cells (green cells) expressing HA-CBP (either FL or Δ Mdm2, red cells) in NIH3T3 (control cells, C) or H-Ras V12 and N-Ras V12 cells is shown at the bottom part of the figure. White arrows indicate transfected cells with undetectable levels of HA-CBP. Data were obtained after counting at least 200 transfected (green) cells from three independent experiments. (B) NIH3T3 H-Ras V12 cells were transfected with 6 μ g of control siRNA duplexes or siRNA duplexes specific for Mdm2 protein. Total cell extracts were prepared 80 hr after transfection and the levels of Mdm2 and CBP/p300 were analyzed by immunoblotting. The diagrams show the relative protein levels obtained from two independent experiments. (C) Total cells extract from NIH3T3 (control cells, C) or H-Ras V12, K-Ras V12 or N-Ras V12 overexpressing cells were analyzed by immunoblot for the presence of Mdm2 using a specific antibody directed against Mdm2. This same blot was also probed with anti-tubulin antibody as a loading control.

Figure 1

A



B

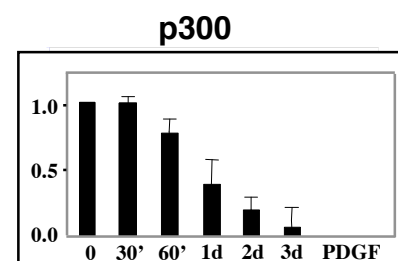
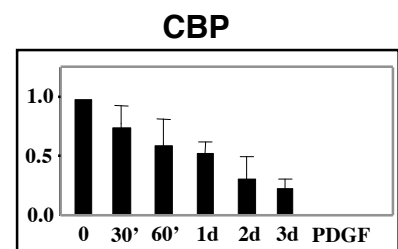
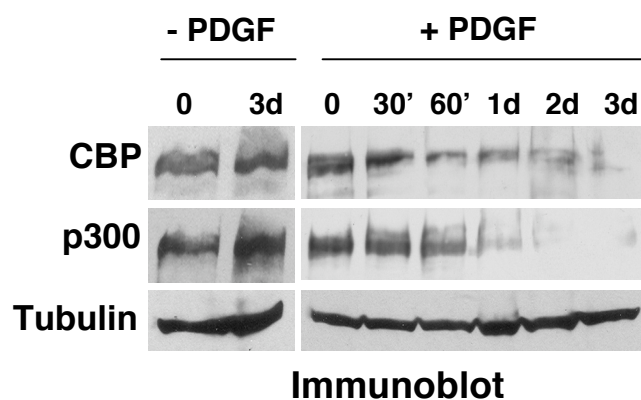


Figure 2

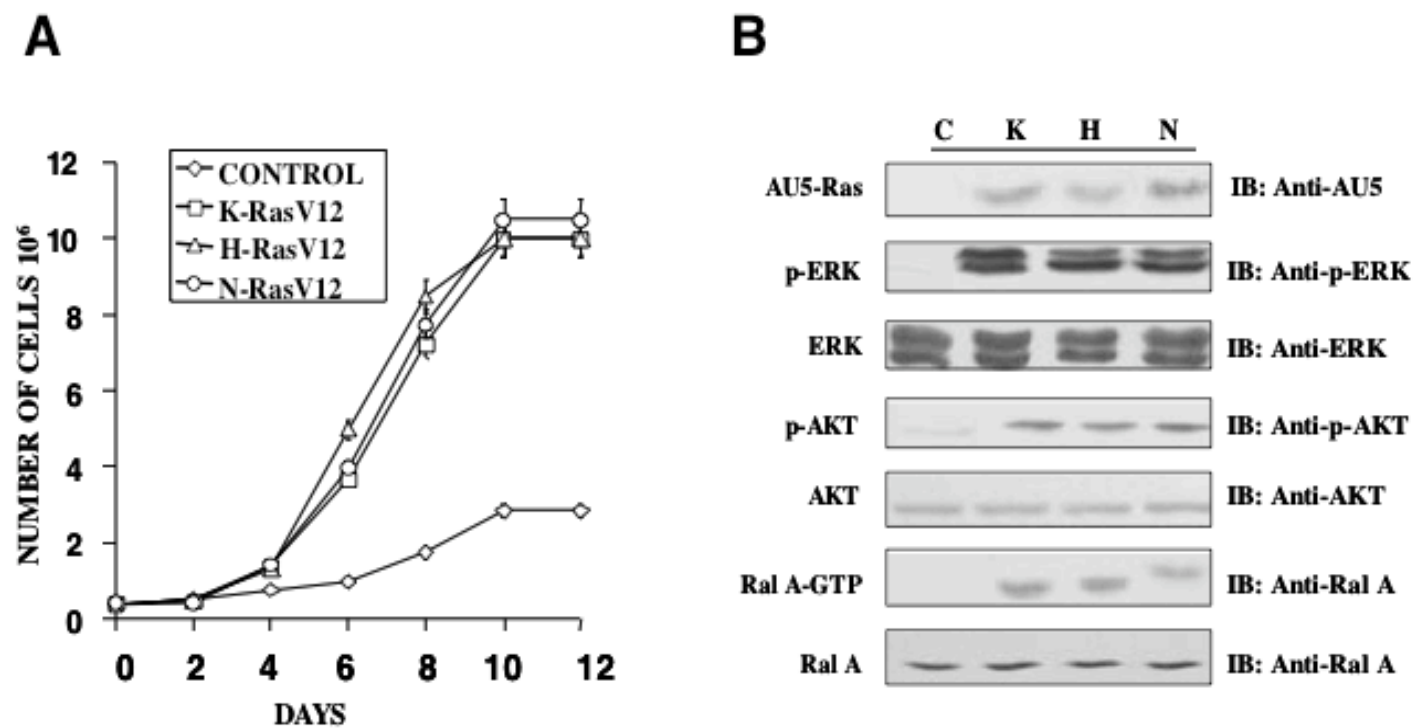
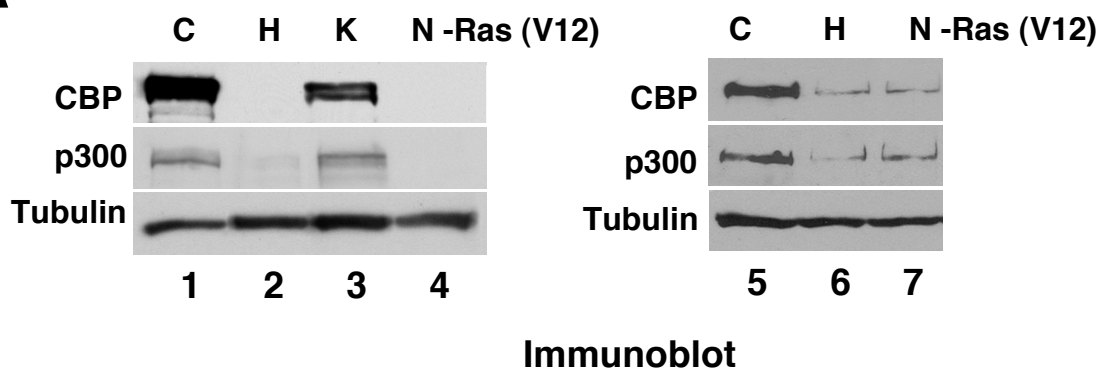
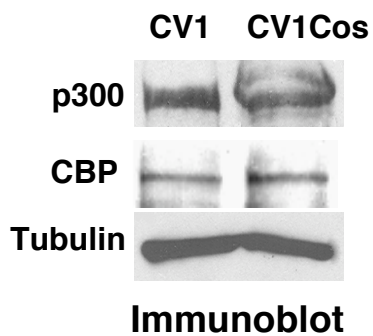


Figure 3

A



B



C

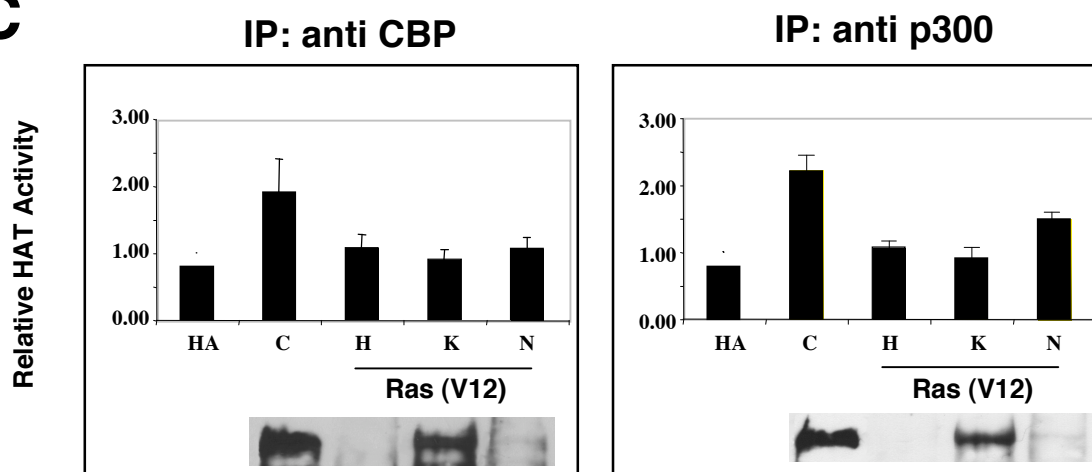
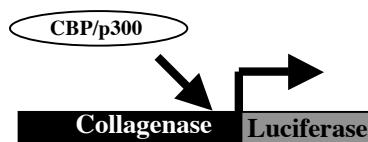
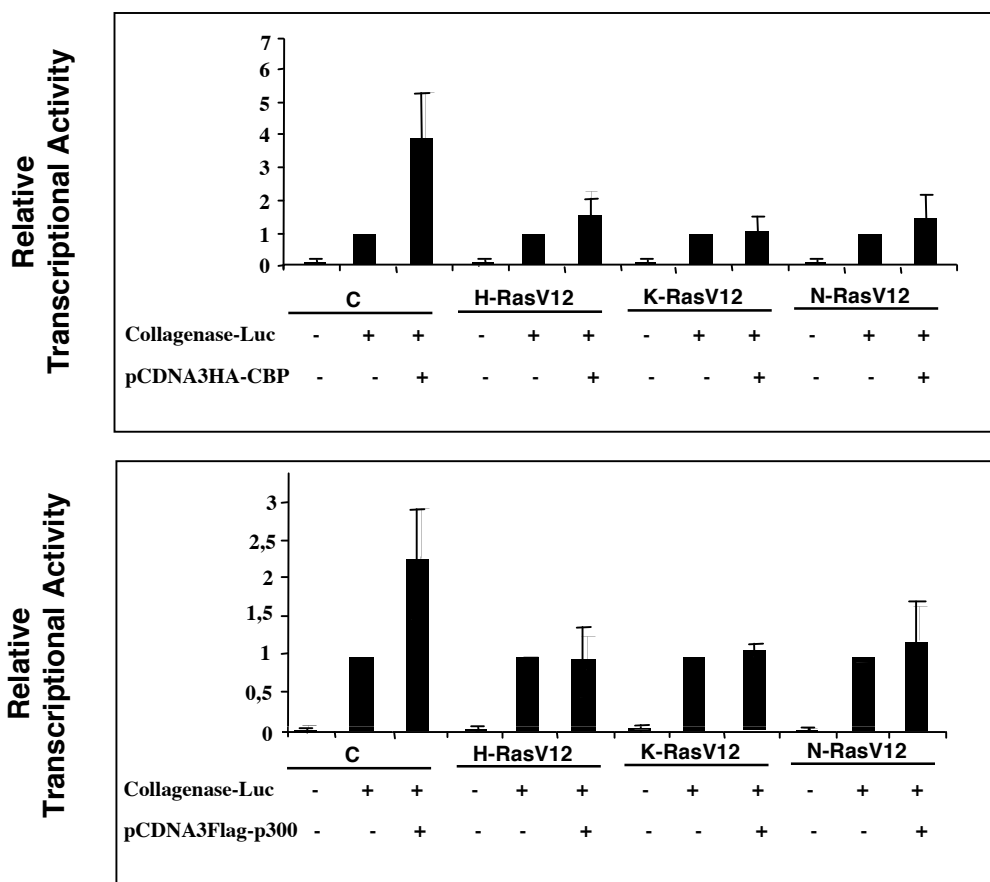


Figure 3

D



E

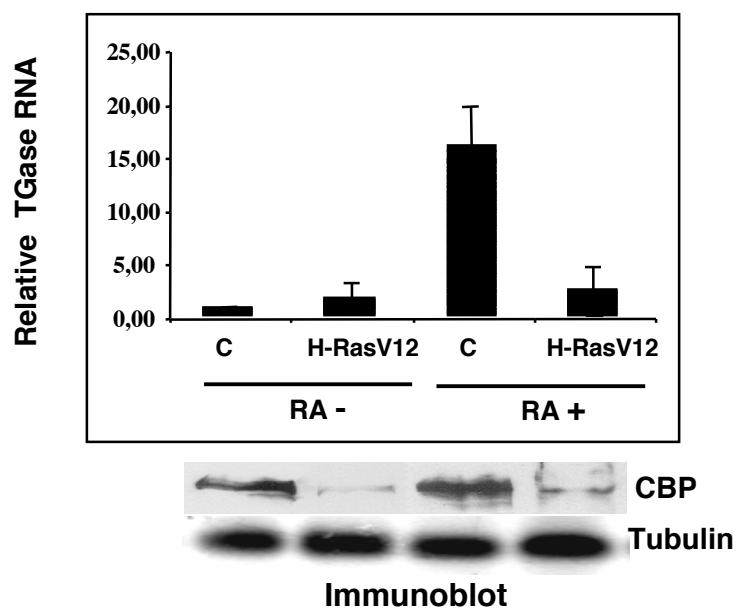
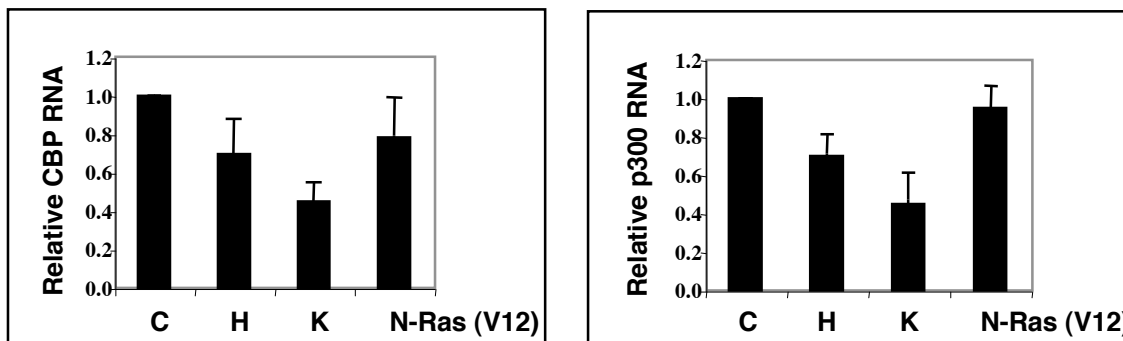
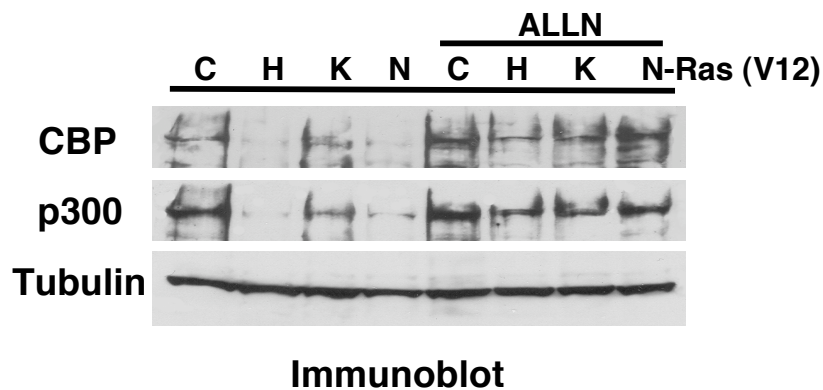


Figure 4

A



B



C

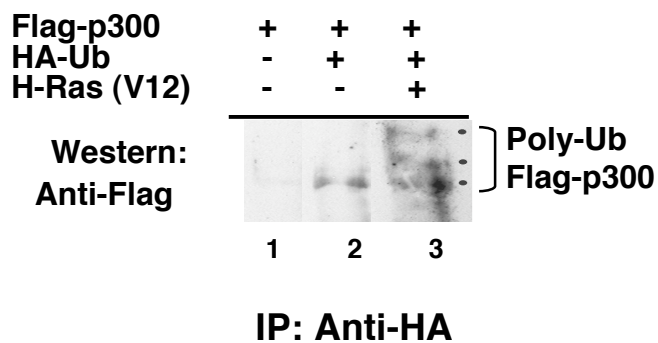
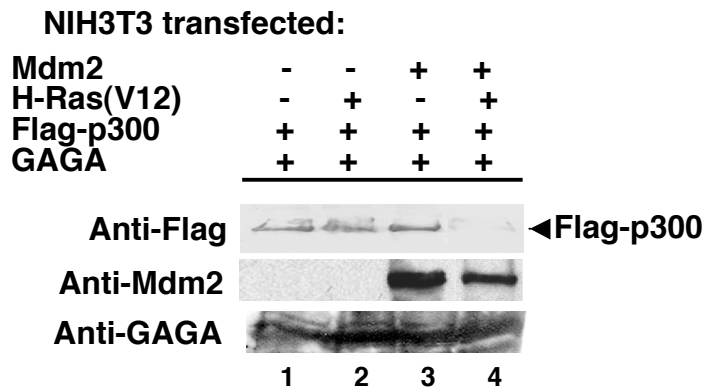


Figure 5

A



B

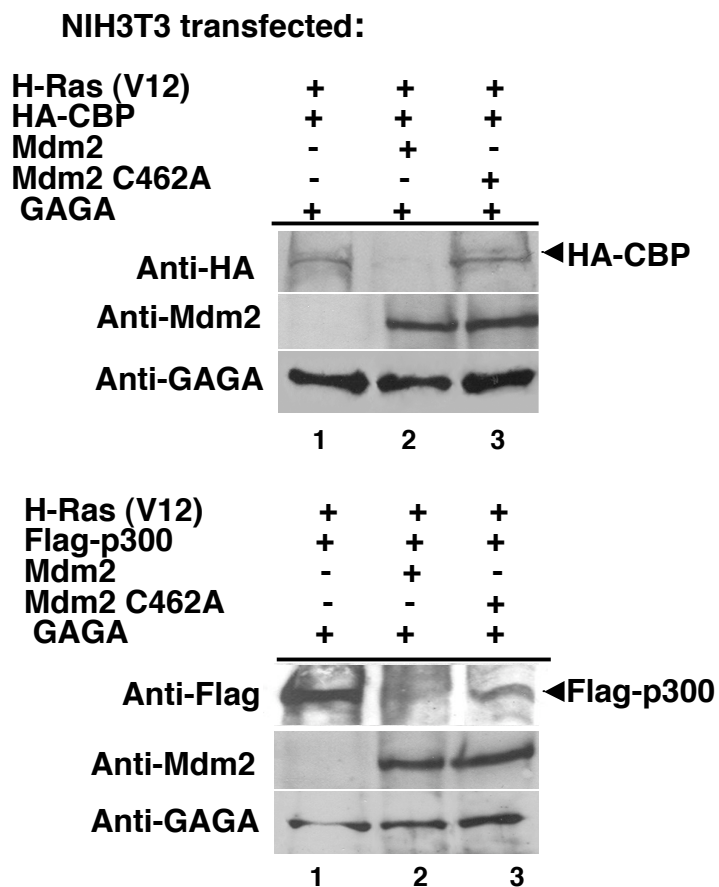
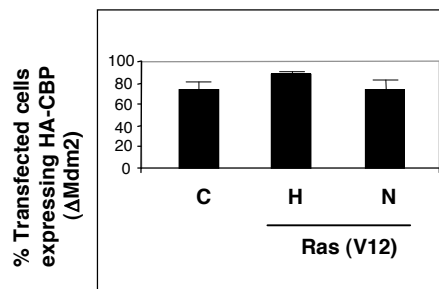
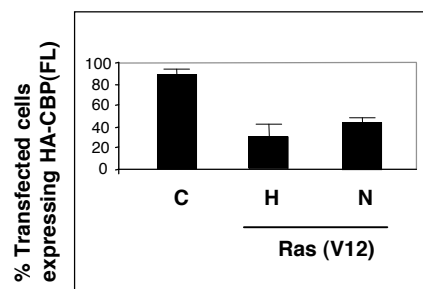
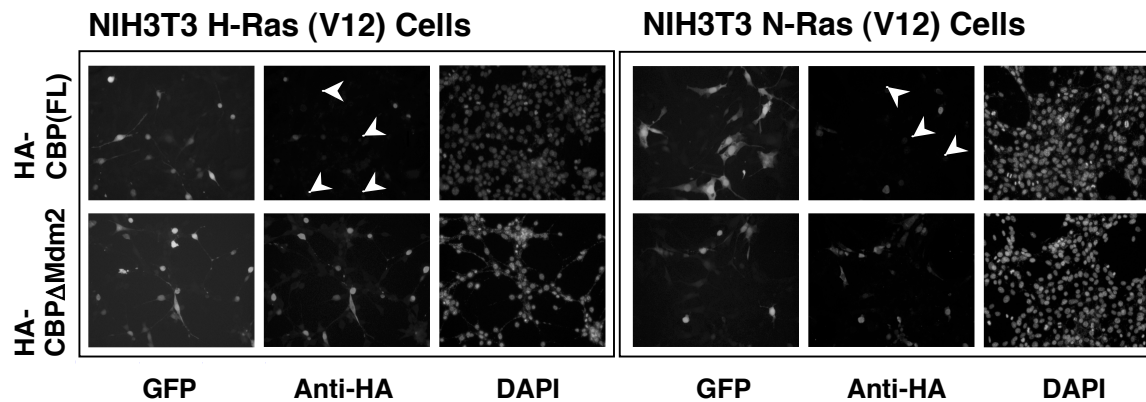
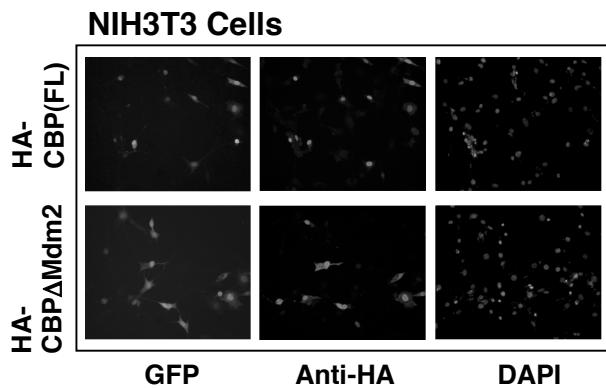
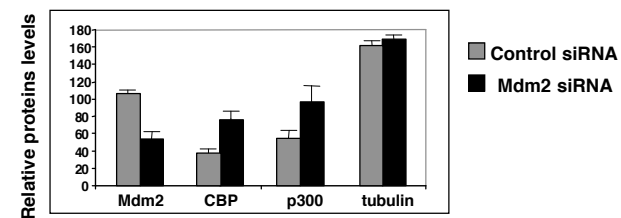


Figure 6

A



B



C

